



Cross-Neutralization of Emerging SARS-CoV-2 Variants of Concern by Antibodies Targeting Distinct Epitopes on Spike

 Siriruk Changrob,^{a,*}
 Yanbin Fu,^{a,§}
 Jenna J. Guthmiller,^a
 Peter J. Halfmann,^b
 Lei Li,^{a,◇}
 Christopher T. Stamper,^{a,c}
 Haley L. Dugan,^{a,c}
 Molly Accola,^d
 William Rehrauer,^{d,e}
 Nai-Ying Zheng,^{a,∞}
 Min Huang,^a
 Jiaolong Wang,^a
 Steven A. Erickson,^a
 Henry A. Utset,^a
 Hortencia M. Graves,^a
 Fatima Amanat,^f
 D. Noah Sather,^{g,h,i}
 Florian Krammer,^f
 Yoshihiro Kawaoka,^{b,j}
 Patrick C. Wilson^{a,c,¶}

^aUniversity of Chicago Department of Medicine, Section of Rheumatology, Chicago, Illinois, USA

^bInfluenza Research Institute, Department of Pathobiological Sciences, School of Veterinary Medicine, University of Wisconsin—Madison, Madison, Wisconsin, USA

^cCommittee on Immunology, University of Chicago, Chicago, Illinois, USA

^dUW Health Clinical Laboratories, University of Wisconsin Hospital and Clinics, Madison, Wisconsin, USA

^eDepartment of Pathology and Laboratory Medicine, University of Wisconsin—Madison, Madison, Wisconsin, USA

^fDepartment of Microbiology, Icahn School of Medicine at Mount Sinai, New York, New York, USA

^gCenter for Global Infectious Disease Research, Seattle Children's Research Institute, Seattle, Washington, USA

^hDepartment of Pediatrics, University of Washington, Seattle, Washington, USA

ⁱDepartment of Global Health, University of Washington, Seattle, Washington, USA

^jDivision of Virology, Department of Microbiology and Immunology, Institute of Medical Science, University of Tokyo, Tokyo, Japan

Siriruk Changrob, Yanbin Fu, and Jenna J. Guthmiller contributed equally. First authorship order was determined based on seniority of the project.

ABSTRACT Several severe acute respiratory syndrome coronavirus 2 (SARS-CoV-2) variants have arisen that exhibit increased viral transmissibility and partial evasion of immunity induced by natural infection and vaccination. To address the specific antibody targets that were affected by recent viral variants, we generated 43 monoclonal antibodies (mAbs) from 10 convalescent donors that bound three distinct domains of the SARS-CoV-2 spike. Viral variants harboring mutations at K417, E484, and N501 could escape most of the highly potent antibodies against the receptor binding domain (RBD). Despite this, we identified 12 neutralizing mAbs against three distinct regions of the spike protein that neutralize SARS-CoV-2 and variants of concern (VOCs), including B.1.1.7 (alpha), P.1 (gamma), and B.1.617.2 (delta). Notably, antibodies targeting distinct epitopes could neutralize discrete variants, suggesting that different variants may have evolved to disrupt the binding of particular neutralizing antibody classes. These results underscore that humans exposed to the first pandemic wave of prototype SARS-CoV-2 possess neutralizing antibodies against current variants and that it is critical to induce antibodies targeting multiple distinct epitopes of the spike that can neutralize emerging variants of concern.

IMPORTANCE We describe the binding and neutralization properties of a new set of human monoclonal antibodies derived from memory B cells of 10 coronavirus disease 2019 (COVID-19) convalescent donors in the first pandemic wave of prototype SARS-CoV-2. There were 12 antibodies targeting distinct epitopes on spike, including two sites on the RBD and one on the N-terminal domain (NTD), that displayed cross-neutralization of VOCs, for which distinct antibody targets could neutralize discrete variants. This work underlines that natural infection by SARS-CoV-2 induces effective cross-neutralization against only some VOCs and supports the need for COVID-19 vaccination for robust induction of neutralizing antibodies targeting multiple epitopes of the spike protein to combat the current SARS-CoV-2 VOCs and any others that might emerge in the future.

KEYWORDS SARS-CoV-2, humoral immunity, immune memory, infectious disease, monoclonal antibodies, single cell, variants of concern

Citation Changrob S, Fu Y, Guthmiller JJ, Halfmann PJ, Li L, Stamper CT, Dugan HL, Accola M, Rehrauer W, Zheng N-Y, Huang M, Wang J, Erickson SA, Utset HA, Graves HM, Amanat F, Sather DN, Krammer F, Kawaoka Y, Wilson PC. 2021. Cross-neutralization of emerging SARS-CoV-2 variants of concern by antibodies targeting distinct epitopes on spike. *mBio* 12:e02975-21. <https://doi.org/10.1128/mBio.02975-21>.

Editor Barry R. Bloom, Harvard School of Public Health

Copyright © 2021 Changrob et al. This is an open-access article distributed under the terms of the [Creative Commons Attribution 4.0 International license](https://creativecommons.org/licenses/by/4.0/).

Address correspondence to Patrick C. Wilson, pcw4001@med.cornell.edu.

*Present address: Siriruk Changrob, Drukier Institute for Children's Health, Weill Cornell Medicine, New York, New York, USA.

§Present address: Yanbin Fu, Drukier Institute for Children's Health, Weill Cornell Medicine, New York, New York, USA.

◇Present address: Lei Li, Drukier Institute for Children's Health, Weill Cornell Medicine, New York, New York, USA.

∞Present address: Nai-Ying Zheng, Drukier Institute for Children's Health, Weill Cornell Medicine, New York, New York, USA.

¶Present address: Patrick C. Wilson, Drukier Institute for Children's Health, Weill Cornell Medicine, New York, New York, USA.

Received 4 October 2021

Accepted 15 October 2021

Published 16 November 2021

The emergence of novel circulating severe acute respiratory syndrome coronavirus 2 (SARS-CoV-2) variants of concern (VOCs) has recently proven to undermine the protective effects of infection- and vaccination-induced humoral immunity (1–4). All approved vaccines against SARS-CoV-2 drive a neutralizing antibody response against the spike protein, the major target of neutralizing antibodies elicited by natural infection (3, 5). However, protective humoral immunity against the spike protein induced by vaccination or infection with the original wild-type (WT) virus may be attenuated due to the widespread circulation of variants (2). The first reported mutation of the SARS-CoV-2 spike protein, D614G, arose in the C-terminal domain (CTD) and evolved due to increased stability of the spike rather than a mutation to escape host immunity (6). More recently, mutations have arisen within the receptor binding domain (RBD), the N-terminal domain (NTD) of S1, and S2 that have resulted in the emergence of several circulating viral variants that are rapidly becoming the dominant strains around the globe (2). The B.1.1.7 lineage or alpha VOC, first found in the United Kingdom, has been reported to have >50% increased transmissibility among humans (7–10). Of the greatest concern is the substitution at position 484 in the RBD, which is exclusively shared by the VOCs, variants of interest (VOIs), and variants under monitoring (VUMs) originally identified in South Africa (B.1.351 [beta]), Brazil (P.1 [gamma]), Texas (R.1), Colombia (B.1.621 [mu]), New York (B.1.526 [iota]), and India (B.1.617.1 [kappa]) (2, 3, 11–15). VOCs possessing a mutation at E484, either E484K or E484Q, can partially evade neutralizing humoral immunity induced by either natural infection or vaccination and, in rare cases, can lead to reinfection or infection, respectively (11–13, 16–18). Other emerging variants have acquired a mutation of L452R within the RBD, which is found in B.1.1.298, a variant capable of interspecies transmission between humans and minks, and B.1.427/B.1.429 (epsilon) isolated in southern California (19). Moreover, B.1.617.1 (kappa) found in India possesses both L452R and E484Q mutations within the RBD (15, 20). The most recent VOC, B.1.617.2 (delta), is responsible for a surge in both cases and fatalities in several countries, especially where vaccination rates are low (4, 21–23). Intriguingly, the B.1.617 lineages contain P681R, a mutation that enhances and accelerates viral fusion (24) and is also present in the dominant variant in Uganda, A.23.1 (25). Thus, understanding the impact of these various mutations on the neutralization capacity of antibodies elicited by current vaccine formulations or natural exposure to WT SARS-CoV-2 is urgently needed to lay the foundation for next-generation vaccine strategies against SARS-CoV-2 variants.

Here, we report that natural WT SARS-CoV-2 infection induces memory B cells expressing potentially neutralizing antibodies against VOCs. Moreover, natural WT infection largely induced antibodies against spike epitopes outside the RBD, most of which were non-neutralizing against the WT and VOCs. Additionally, RBD binding antibodies could be categorized into 3 distinct classes based on their binding profiles against RBD mutant constructs. We identified VOC-neutralizing antibodies against three distinct regions of the spike protein, including two epitopes on the RBD and one epitope in the NTD. Together, our study identifies that natural WT infection induces memory B cells that can produce neutralizing antibodies against recent SARS-CoV-2 VOCs and have the potential to be recalled by vaccination.

RESULTS

Convalescent-phase sera have reduced antibody titers but retain neutralization capabilities against circulating SARS-CoV-2 VOCs. To investigate whether antibodies from subjects naturally infected with WT SARS-CoV-2 lost binding or neutralization activity against VOCs, we collected blood samples from 10 convalescent donors at a median of 49 days after symptom onset (26, 27) (see Table S1 in the supplemental material) for an in-depth analysis of the specificity of individual memory B cells. As an initial estimate of antibody activity from these patients, serum antibody reactivity was measured by comparing reactivities to WT trimeric SARS-CoV-2 spike and spike proteins from the D614G, B.1.1.7, B.1.351, P.1, B.1.617.2, B.1.526, and B.1.617.1 variants. While serum antibody IgG titers from these 10 patients against WT and D614G spike antigens

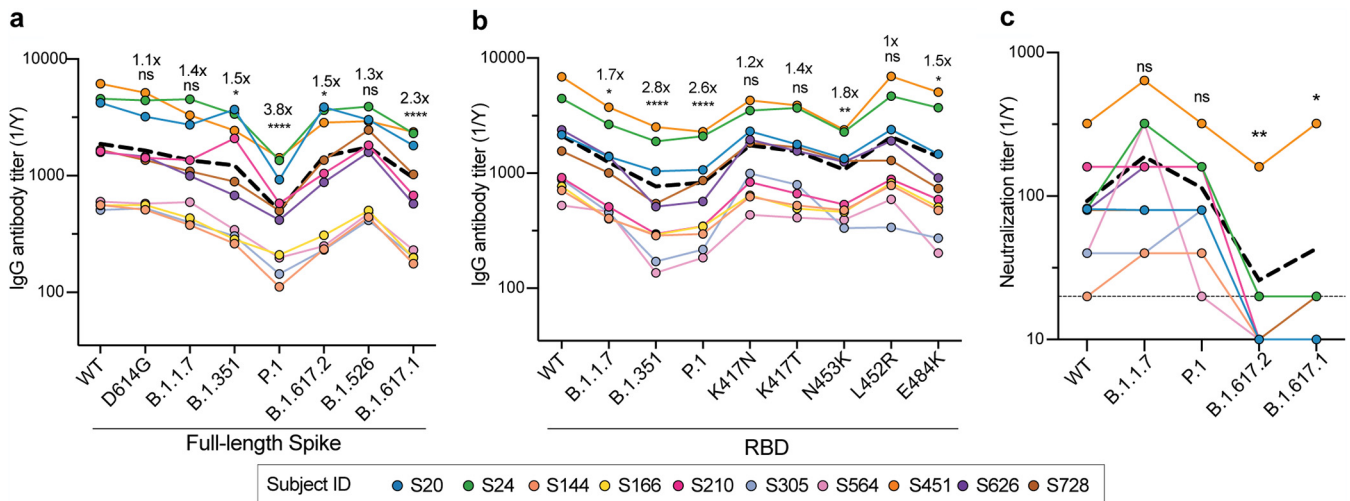


FIG 1 Analyses of serum antibody responses in COVID-19 convalescent individuals. (a and b) Total IgG endpoint antibody titers from 10 convalescent subjects against SARS-CoV-2 full-length spike variants (a) and RBD recombinant antigens (b). The dashed line is the mean IgG titer. (c) Neutralization titers from 10 convalescent donors against WT SARS-CoV-2, B.1.1.7, P.1, B.1.617.2, and B.1.617.1. The dashed line represents the mean neutralization titer. Data in panels a to c were analyzed using nonparametric Friedman's test with Dunnett's multiple-comparison test. Fold changes in relative mAb binding to variants or mutants compared to the WT in panels a and b are indicated above the statistical asterisks. ns, not significant.

were similar, titers were significantly reduced against the spike proteins of B.1.1.7 (1.4-fold), B.1.351 (1.5-fold), P.1 (3.8-fold), B.1.617.2 (1.5-fold), B.1.526 (1.3-fold), and B.1.617.1 (2.3-fold) relative to the WT spike protein (Fig. 1a). Similarly, IgG titers against the RBDs of B.1.1.7 (1.7-fold), B.1.351 (2.8-fold), and P.1 (2.6-fold) were reduced compared to those against the WT RBD. However, we noted that there was less than a 2-fold decrease in antibody binding against single mutants of the RBD (Fig. 1b). Despite reductions in serum binding activity, the sera retained similar neutralizing titers against the WT and the B.1.1.7 and P.1 SARS-CoV-2 variants. However, we found a significant reduction in neutralization against B.1.617.1 and B.1.617.2 compared to the WT (Fig. 1c). Although antibody titers were lower against the VOCs and VUMs, these data indicate that serum antibodies elicited by natural WT infection were able to neutralize B.1.1.7, P.1, and WT viruses equally, while most donors lost neutralizing potential against B.1.617 lineage viruses.

Generation of mAbs against distinct domains of the SARS-CoV-2 spike. We next sought to determine the specificities of antibodies that could cross-neutralize these viral variants by generating monoclonal antibodies (mAbs) from spike binding B cells isolated from 10 convalescent subjects, collected between April and July 2020 (26, 27). We sorted B cells binding to spike and/or RBD fluorophore- and oligonucleotide-conjugated probes and performed single-cell RNA sequencing (RNA-seq) and B cell receptor sequencing. As the antigen probes included a DNA oligonucleotide sequence, we were able to track the antigen specificity of isolated B cells. In total, we obtained 1,703 paired immunoglobulin heavy and light chains from non-RBD and RBD binding B cells specific for the spike. Overall, the percentage of spike non-RBD binding B cells was 4-fold higher than that of RBD binding B cells (Fig. 2a to c), indicating that natural WT infection preferentially induced B cell responses to epitopes on the spike outside the RBD (28, 29). Overall, B cells targeting the RBD or epitopes outside the RBD utilized similar V(D)J genes, had overlapping heavy and light chain pairings, and possessed similar numbers of mutations and complementarity-determining region 3 (CDR3) lengths (Fig. S1a to i).

Based on the acquired antibody sequences and probe binding intensities, we generated 43 mAbs from all 10 donors specific for the WT spike protein (Table S2). To investigate specific domain targeting, mAbs were tested for binding to the RBD and monomeric S1 and S2 recombinant spike antigens. Based on binding to these discrete antigens, spike-reactive mAbs were categorized into 4 groups: NTD-A-reactive mAbs

($n = 5$) that bound strongly to S1 but not the RBD, NTD-B-reactive mAbs ($n = 7$) that weakly bind S1 but not the RBD, S2-reactive mAbs ($n = 2$), and RBD-reactive mAbs ($n = 29$) (Fig. 2d and e). Additionally, NTD-A- and NTD-B-classified antibodies targeted distinct epitopes as shown by a competition enzyme-linked immunosorbent assay (ELISA) (Fig. S2a). We further determined whether antibodies with different binding specificities differ in their neutralization capacities against WT SARS-CoV-2. Of the 43 mAbs, 18 (42%) were neutralizing. Notably, only mAbs binding the RBD and NTD-B were neutralizing, whereas all mAbs binding NTD-A and S2 were non-neutralizing (Fig. 2d to f). Moreover, 52% of RBD-targeting mAbs were neutralizing, with eight mAbs being potently neutralizing antibodies (50% inhibitory concentration [IC_{50}] of <500 ng/ml) and three out of seven NTD-B mAbs having moderate neutralization potency (5,000 to 7,500 ng/ml) (Fig. 2g and h). Of the 10 convalescent donors, 7 had at least one neutralizing mAb among the antibodies cloned for this study, although the potencies of the mAbs varied by donor (Fig. 2i). Together, these data reveal that mAbs against the RBD are the predominant source of neutralizing antibodies induced by WT SARS-CoV-2 infection.

Binding and neutralizing breadth of non-RBD spike antibodies. To understand the effects of viral variants on mAb binding to epitopes on the spike outside the RBD, we tested non-RBD-targeting mAbs for binding to a panel of SARS-CoV-2 variants, including D614G and the emerging variants B.1.1.7, B.1.351, P.1, B.1.617.2, B.1.526, and B.1.617.1 (Fig. 3a to g). All non-RBD spike-reactive antibodies showed similar binding to the D614G spike. Furthermore, all mAbs targeting NTD-A and S2 maintained similar binding to the spike of the B.1.1.7, B.1.351, P.1, B.1.617.2, B.1.526, and B.1.617.1 variants (Fig. 3h). Although mAbs against NTD-A and S2 retain binding to VOCs, they are non-neutralizing, implying that NTD-A- and S2-reactive antibodies may provide limited immune pressure to mutate these epitopes. Of interest, NTD-B mAbs showed significantly reduced binding to the spike of B.1.1.7, B.1.351, B.1.617.2, and B.1.617.1 while showing similar binding to B.1.526 and a minor reduction in binding to the spike of P.1 (Fig. 3h). Two of the three neutralizing NTD-B binding mAbs (S166-32 and S305-1456), which were isolated from two different subjects, retained neutralization potential against B.1.1.7 and P.1 at moderate neutralizing potency (Fig. 3h). The third neutralizing NTD-B binding mAb (S24-1301) also had moderate neutralizing potency against the WT strain, with weak cross-neutralization activity against the P.1 variant and no neutralization activity against B.1.1.7, consistent with its binding profile (Fig. 3h). However, all three neutralizing NTD-B mAbs failed to neutralize B.1.617.1 and B.1.617.2. Together, our data indicate that antibodies against NTD-B show cross-neutralization capacity and thus may provide protection against some emerging VOCs such as B.1.1.7 and P.1. However, antibodies targeting the NTD-B epitope may be driving spike evolution, particularly the mutations and deletions found within B.1.1.7, B.1.351, B.1.617.1, and B.1.617.2, leaving the future of this epitope as a reliable target for cross-reactive antibodies uncertain.

A subset of RBD-binding mAbs retains neutralization activity against VOCs. Viral escape mutations occurring within the RBD may result in a reduction of the neutralization capacity of RBD-targeting antibodies (30–32). To understand the impacts of RBD mutations on mAb binding, we tested RBD-targeting mAbs for binding to RBD mutants that possessed a single mutation found in circulating SARS-CoV-2 VOCs, VOIs, VUMs and artificial mutants at key contact residues of the RBD-ACE2 interaction (30–35) as well as full-length (FL) spike constructs containing multiple mutations in the RBD (Table S3). In addition, we tested mAb binding to the RBDs of SARS-CoV-1 and Middle East respiratory syndrome coronavirus (MERS-CoV) to investigate cross-reactivity to other coronaviruses. Notably, RBD binding mAbs have been classified into four

FIG 2 Legend (Continued)

in panels h and i are colored based on domain specificity, and the dashed lines shown in panels h and i indicate the limit of detection (10,000 ng/ml). Data in panels d to i are representative of results from two independent experiments performed in duplicate. Genetic characterization of each mAb is further detailed in Table S2 in the supplemental material.

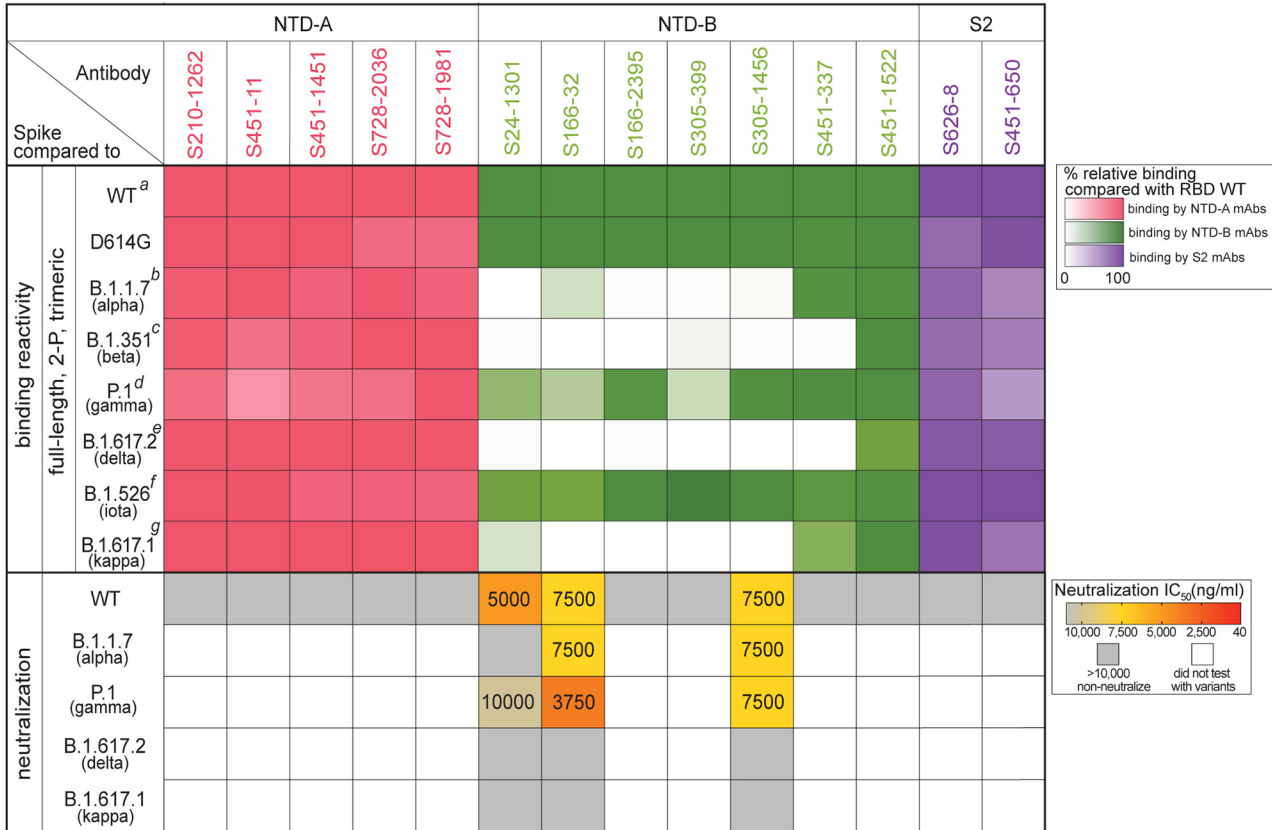
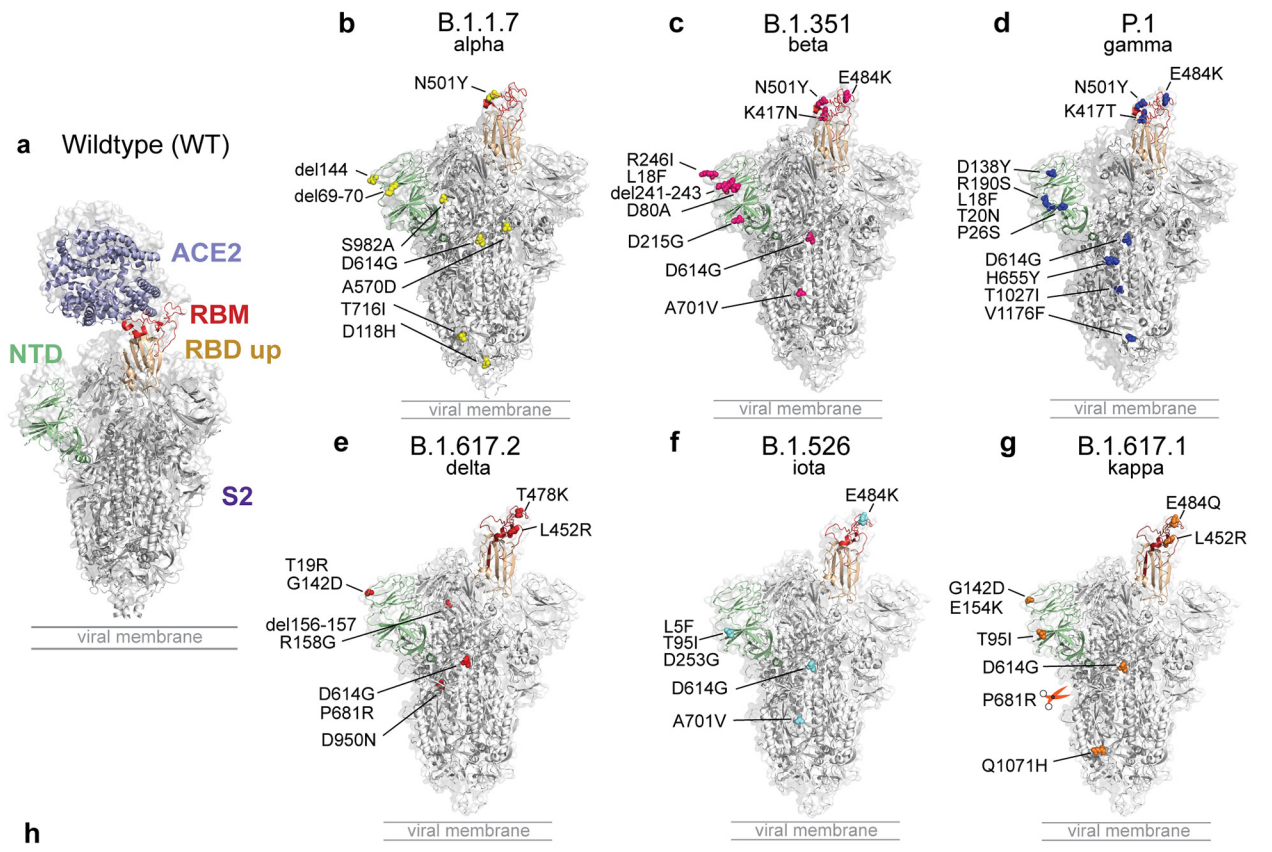


FIG 3 Binding breadth and neutralization of spike non-RBD mAbs. (a) Full-length spike protein binding to ACE2 (PDB accession number 7KJ2). (b to g) Locations of mutations found on B.1.1.7 (b), B.1.351 (c), P.1 (d), B.1.617.2 (e), B.1.526 (f), and B.1.617.1 (g) (modified from the structure under (Continued on next page)

classes, classes 1 to 4 or receptor binding sites (RBSs) A to D, based on structural analysis and antibody binding features (36, 37). More recently, the classification of four key antigenic regions of the RBD can also be defined by determining the loss of binding to RBD mutants (class 1 to 3 epitopes) or binding to cryptic epitopes on the RBD that are conserved across SARS-CoV-1 and MERS-CoV RBDs (class 4 epitope) (Fig. 4a and b) (17, 30). Based on the binding profiles of class 1 to 4 binding mAbs, we were able to segregate 23 out of 29 mAbs into one of the four classes (Fig. 4c and Fig. S2b). Notably, no class 1 mAbs were found and six mAbs could not be classified as they either lost binding to multiple mutant classes or bound equally to all RBD mutants but did not bind to SARS-CoV-1 or MERS-CoV.

Class 2 RBD binding mAbs showed reduced binding to at least one of the RBD class 2 single escape mutants, notably E484K and F490K, and the majority of these mAbs lost binding to the RBD mutants found in B.1.351, P.1, B.1.526, and B.1.617.1 (Fig. 4c). Of the 12 class 2 mAbs, 11 were potently neutralizing against WT SARS-CoV-2. Of the neutralizing class 2 mAbs, all but one neutralized B.1.1.7 at concentrations comparable to those for neutralization of the WT strain. In contrast, six mAbs neutralized B.1.617.2 at a lower potency than for the WT and B.1.1.7. Seven of the class 2 mAbs retained their neutralization activity against at least two VOCs (Fig. 4c). Of note, 10 out of 11 neutralizing class 2 mAbs were unable to neutralize the variants that harbored a mutation at E484, P.1 and B.1.617.1. This is in line with previous studies that showed that the E484K and E484Q mutations are the key escaping residues responsible for neutralization resistance by P.1, P.2, B.1.351, and B.1.617.1 VOCs (2, 4, 38). Of the greatest interest, S144-1406, which retained binding to E484K and all spike variants, neutralized B.1.1.7 and P.1 variants with high neutralization potency. Similar to another E484K binder, S24-1224 neutralized three out of four VOCs tested, including B.1.617.1 (Fig. 4c). These data indicate that some class 2 antibodies can cross-neutralize VOCs. Additionally, the epitope targeted by S144-1406 partially overlapped the ones targeted by S24-1224 and other class 2 mAbs that failed to neutralize P.1 and B.1.617.1 (Fig. S2c), suggesting that class 2 mAbs target similar but slightly different RBD epitopes.

Only one mAb (S24-821) specifically lost binding to the class 3 mutants, particularly to N439K and N440K, which are associated with circulating SARS-CoV-2 variants (35, 39) and have been reported as *in vitro* escape sites for class 3 epitope binding mAbs (30, 31, 35) (Fig. 4b and Table S3). Moreover, we classified five more mAbs as class 3-like as they strongly competed for RBD binding with S24-821 but did not compete with class 2 mAbs (Fig. S2b). Importantly, all class 3 and class 3-like mAbs maintained binding to L452R, another mutation associated with class 3 antibodies that is present in B.1.427/B.1.429 (19, 40) and B.1.617 (20) variants (Fig. 4c). However, there was a 2- to 3-fold reduction of class 3 and class 3-like mAbs in binding against B.1.617.2 that carries T487K and L452R substitutions in the RBD region. Of the four neutralizing class 3 and class 3-like mAbs, all four retained neutralization activity against B.1.1.7, and three were neutralizing against P.1 (Fig. 4b). In contrast to class 2 mAbs, B.1.617.2 was resistant to all class 3-neutralizing mAbs. Only one mAb (S24-821) retained modest neutralization potency against B.1.617.1, indicating that antibodies binding class 3 epitopes could neutralize some VOCs even though they bound the L452R single mutation and all spike variants.

All of the mAbs that were categorized into class 4 ($n = 5$) maintained binding to all RBD mutants and spike variants and displayed cross-reactivity to the SARS-CoV-1 RBD. However, all class 4 mAbs were non-neutralizing against WT virus, suggesting that antibodies against this epitope are likely not strong drivers of antigenic drift. Notably,

FIG 3 Legend (Continued)

PDB accession number 6XM4). (h) Binding reactivity and neutralization capabilities of NTA-A (pink), NTD-B (green), and S2 (purple)-reactive mAbs. The color gradients indicate the percentages of relative binding compared to WT spike. The neutralization potencies (IC_{50}) of spike non-RBD mAbs against the WT and the B.1.1.7, P.1, B.1.617.2, and B.1.617.1 variants are indicated in nanograms per milliliter. The panel of SARS-CoV-2s is detailed in Table S4 in the supplemental material. Data in panel h are representative of results from two independent experiments performed in duplicate. Genetic information for each mAb can be found in Table S2.

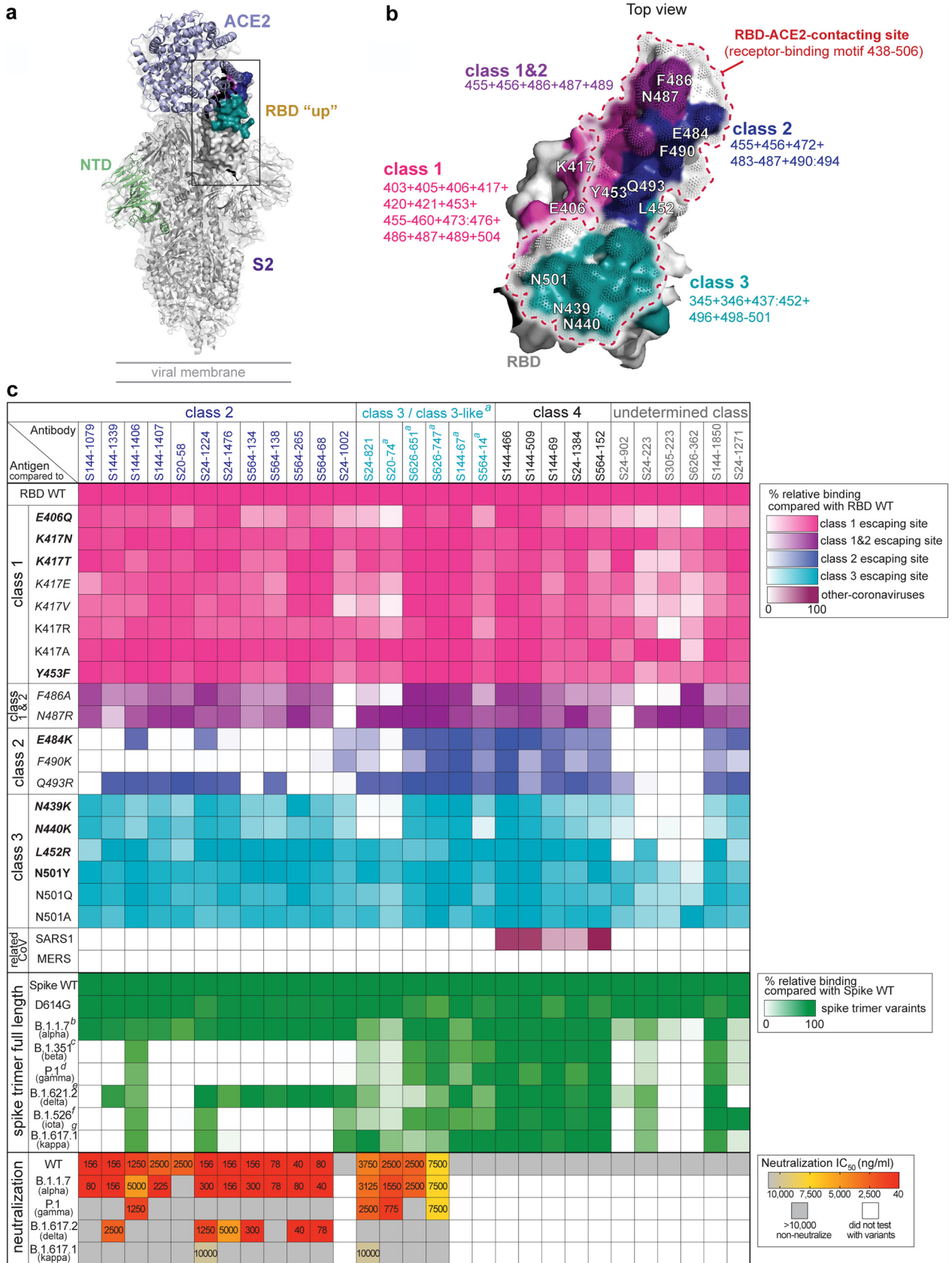


FIG 4 Binding and neutralization profiles of RBD binding mAbs against a panel of RBD escape mutants and variants. (a) Structural model of RBD “up” binding with ACE2 (PDB accession number 7KJ2) and RBD antibody classes and associated escape mutants. (b) RBD colored by antibody (Continued on next page)

three antibodies in the class 4 group utilized the same heavy chain gene, VH5-51, as CR3022 and competed with CR3022 for binding to the RBD, indicating that the class 4 antibodies in our study likely target the same or a similar epitope as CR3022 (Table S2 and Fig. S2d). This is consistent with a previous study showing that CR3022 cross-reacts with SARS-CoV-1, suggesting that class 4 antibodies are common across subjects and studies (17, 30).

With the classification of mAbs against distinct epitopes, we next tested the relative abundances of serum antibodies against these distinct epitopes of the RBD and NTD by performing competition assays. Notably, donors had significantly higher titers of serum antibodies targeting class 3 (S24-821) and class 3-like (S20-74) epitopes, whereas subjects largely had undetectable titers against class 2 and NTD-B epitopes, suggesting that WT SARS-CoV-2 infection predominantly induces polyclonal antibodies targeting RBD class 3 epitopes that can neutralize the emerging VOCs B.1.1.7 and P.1 (Fig. S2e). These data are consistent with the observed anti-B.1.1.7 and anti-P.1 serum neutralizing titers shown in Fig. 1c, suggesting that the retention of serum neutralization activity could be due to abundant class 3 antibody responses. The loss of neutralization capabilities against B.1.617 lineage viruses may be due to insufficient levels of class 2 serum antibodies. A comparison of the neutralization capabilities of mAbs targeting different epitopes revealed that class 2 RBD-reactive mAbs were the most potently neutralizing, followed by mAbs targeting class 3 RBD epitopes and NTD-B (Fig. S3a). It is important to note that none of neutralizing mAbs induced by natural WT infection were able to neutralize all emerging SARS-CoV-2 variants. Nonetheless, we identified at least one mAb that could neutralize each VOC, suggesting that the convalescent donors generated a diverse cross-neutralizing antibody response (Fig. S3b). Therefore, antibodies targeting multiple epitopes on the spike are a valuable source of neutralizing antibodies against emerging VOCs. Additionally, we found that the majority of antibodies isolated from donors who had high antibody titers exhibited lower neutralizing potency than antibodies derived from donors who had lower serological titers and less severity (Fig. S3b and Table S1). However, there was no difference between high and low responders in generating cross-neutralizing antibodies against VOCs and VUMs. Moreover, the cross-neutralizing RBD-targeting mAbs used V(D)J gene features similar to those for other previously reported RBD binding mAbs (Table S3) (41–43). However, the mAbs in our studies utilized distinct heavy and light chain pairings, indicating that these clones are not public with other known neutralizing SARS-CoV-2 antibodies. Despite this, our data indicate that cross-neutralizing antibodies use a diverse antibody repertoire against multiple distinct epitopes. Therefore, driving a polyclonal antibody response against these three epitopes may provide cross-neutralizing protection against existing and future variants.

DISCUSSION

Our study shows that WT SARS-CoV-2 convalescent individuals possess antibodies that can effectively cross-neutralize emerging VOCs, with cross-neutralizing antibodies targeting multiple epitopes of the spike protein. In total, we identified 12 mAbs that potently neutralize currently circulating VOCs, including B.1.1.7, the alpha variant, which has been reported to be more infectious (8, 19); P.1, the gamma variant, which

FIG 4 Legend (Continued)

classes and associated mutations. Pink, class 1; purple, overlap of classes 1 and 2; blue, class 2; teal, class 3. (c) Heat map detailing the binding reactivity of RBD mAbs ($n = 29$) against single key escape sites for class 1, class 2, and class 3 antibodies; combinations of RBD mutants; and the RBDs from SARS-CoV-1 and MERS-CoV. *a* refers to class 3-like antibodies, which are defined by mAbs that compete with a class 3 mAb (see Fig. S2c in the supplemental material). *b* to *f* refer to mutations in the RBD of each full-length spike variant, B.1.1.7 with N501Y (*b*), B.1.351 with K417N:E484K:N501Y (*c*), P.1 with K417T:E484K:N501Y (*d*), B.1.617.2 with T478K:L452R (*e*), B.1.526 with E484K (*f*), and B.1.617.1 with L452R:E484Q (*g*). The panel of recombinant antigens in panel c is detailed in Table S3, including mutations found in circulating SARS-CoV-2 variants (boldface type), mutations that escape/reduce binding by polyclonal serum/potent neutralizing mAbs (italic type), mutations found in both circulating SARS-CoV-2 variants and the *in vitro* escape map (boldface and italic type), and artificial mutants at key contact residues of the RBD-ACE2 interaction (normal typeface). The neutralization potencies (IC_{50}) of spike RBD mAbs against the WT and the B.1.1.7, P.1, B.1.617.2, and B.1.617.1 variants are indicated in nanograms per milliliter. The panel of SARS-CoV-2s is detailed in Table S4. Data in panel c are representative of results from two independent experiments performed in duplicate. Genetic information for each antibody can be found in Table S2.

partially escapes both natural and vaccine-induced humoral immunity (2, 12, 44); and B.1.617.2, the delta variant, which is more transmissible than the alpha variant, has led to a surge of more hospitalizations in India, and can evade partial immunity induced by one vaccine dose (4, 15, 23). Convalescent subjects in our cohort had sufficient serum titers to neutralize both B.1.1.7 and P.1 but not B.1.617, suggesting that the cross-neutralizing mAbs identified in this study may play an important role in polyclonal neutralization for some of the VOCs.

Using high-throughput antigen probing at the single-B-cell level, we found that B cells isolated from convalescent subjects largely targeted non-RBD epitopes rather than potently neutralizing epitopes on the RBD. Similarly, mRNA vaccines also largely induce antibodies against non-neutralizing epitopes, suggesting that epitopes outside the RBD are immunodominant (3, 45). Despite this, vaccination has been shown to induce cross-neutralizing antibodies (1), suggesting that both natural WT infection and currently approved vaccines can elicit protective humoral immunity against emerging variants. As we identified 12 antibodies cross-neutralizing to VOCs derived from seven different convalescent coronavirus disease 2019 (COVID-19) donors, our study suggests that most people generate a cross-neutralizing antibody response. Notably, these antibodies largely target three distinct epitopes, including two sites on the RBD and one on the NTD. Several recent studies have demonstrated that antibodies against the NTD and S2 are neutralizing (46–48). Although the anti-S2 mAbs identified in our study were non-neutralizing, S2 binding antibodies exhibit broad reactivity with spike proteins from SARS-CoV-2 variants, related betacoronaviruses such as SARS-CoV-1 and MERS-CoV, and distantly related endemic coronaviruses. Moreover, anti-spike serum antibodies can mediate protection via Fc-mediated functions, suggesting that a combination of neutralizing antibodies and polyfunctional antibodies will provide optimal protection against infection with variants of SARS-CoV-2 (49).

Our study also showed that anti-RBD mAbs are primarily class 2 mAbs, consistent with other reports (30, 37, 42, 50). The majority of the class 2 mAbs retained their neutralization activity against B.1.1.7 and B.1.617.2 but were largely non-neutralizing against P.1, suggesting that class 2 mAbs may have driven the evolution of P.1 mutants. In contrast, neutralizing class 3 mAbs retained their neutralization activity against both B.1.1.7 and P.1 but did not neutralize the B.1.617 variants. Notably, none of the neutralizing mAbs could cross-neutralize B.1.1.7, P.1, and B.1.617.2, the most prevalent VOCs as of writing. Therefore, vaccination approaches to increase the affinity and frequencies of antibodies to the S1 domain may enhance the breadth of protection against emerging SARS-CoV-2 VOCs, including epitopes on the RBD and NTD. It is likely that targeting multiple epitopes will provide optimal protection to avoid the generation of escape mutants that can evade antibodies against any one epitope. Moreover, vaccinating previously infected subjects has been shown to substantially improve neutralization titers (3) and may allow refinement of memory B cells against neutralizing epitopes.

In conclusion, our study shows that SARS-CoV-2 infection induces cross-neutralizing immunity against circulating VOCs, which is likely attributed to polyclonal antibodies targeting multiple epitopes of the spike protein. This work emphasizes the need for the induction of cross-neutralizing antibodies that bind distinct sites on the spike with various mechanisms that can synergize to provide protection against SARS-CoV-2 variants as well as limit the virus from escaping any single antibody target.

MATERIALS AND METHODS

Study cohort and spike-specific B cell sorting. All studies were performed with the approval of the University of Chicago institutional review board (IRB20-0523), the University of Chicago, and the University of Wisconsin—Madison. Informed consent was obtained after the research applications and possible consequences of the studies were disclosed to study subjects. This clinical trial was registered at ClinicalTrials.gov under identifier NCT04340050, and clinical information for patients included in the study is detailed in Table S1 in the supplemental material. The details of peripheral blood mononuclear cell (PBMC) collection from leukoreduction filters were described previously (27). For spike-specific B cell sorting, PBMCs were thawed in a 37°C water bath, and B cells were enriched using a human pan-B cell EasySep enrichment kit (Stemcell). B cells were stained with anti-CD19-phycoerythrin (PE)-Cy7

(BioLegend), anti-CD3-BV510 (BD Biosciences), and antigen probes (PE) for 30 min on ice in 1× phosphate-buffered saline (PBS) supplemented with 0.2% bovine serum albumin (BSA) and 2 mM Pierce biotin. Probe generation was performed as previously described (27). Cells were subsequently washed with 1× PBS with 0.2% BSA and stained with Live/Dead BV510 (Thermo Fisher) in 1× PBS for 15 min. Cells were washed again and resuspended at a maximum of 4 million cells/ml in 1× PBS supplemented with 0.2% BSA and 2 mM Pierce biotin for downstream cell sorting using the MACSQuantTyto cartridge sorting platform (Miltenyi). Viable/CD19⁺/antigen-PE-positive cells were sorted as probe positive. Cells were then collected from the cartridge sorting chamber and used for downstream processing with a chromium controller (10X Genomics).

Single-cell RNA-seq and B cell receptor sequencing. The human B cell V(D)J, 5' gene expression, feature barcode libraries were prepared according to the manufacturer's instructions. Libraries were pooled and sequenced using an Illumina NextSeq550 or an Illumina NextSeq 500 platform at the University of Chicago. Cell Ranger (version 3.0.2) was used to perform raw sequence processing, sample demultiplexing, barcode processing, single-cell 5' transcript counting, and B cell receptor repertoire sequence assembly. The reference genome assembly for the transcriptome is GRCh38-1.2.0, and the reference genome assembly for V(D)J is cellranger-*vdj*-GRCh38-alts-ensembl-2.0.0. The data obtained from Cell Ranger were subsequently used for downstream analysis using the Seurat toolkit (version 3.2.0) (an R package for transcriptome, cell surface protein, and antigen probe analyses) (51) and IgBlast (version 1.15) for immunoglobulin gene analysis (52). Cell quality control (QC), normalization, data scaling, linear dimensional reduction, clustering, differential expression analysis, batch effect correction, and data visualization were performed using Seurat (version 3.2.0). QCs of cells were performed further to exclude cells with <200 and >2,500 detected genes and cells expressing a high percentage of mitochondrial genes. Transcriptome RNA data were analyzed using conventional log normalization. We performed a principal-component analysis (PCA) and used the top 15 principal components (PCs) for linear dimensional reduction and clustering. Only filtered, high-quality cells were clustered in this analysis using the Louvain algorithm implemented in Seurat under a resolution of 0.6 for clustering. Batch effects across different data sets were normalized using an Anchor method implemented in Seurat.

Monoclonal antibody production. B cells were selected for mAb generation based on antigen probe intensity visualized by JMP Pro 15, as previously described (27). Antibody heavy and light chain genes obtained by 10X Genomics V(D)J sequencing analysis were synthesized by Integrated DNA Technologies. The synthesized fragments for heavy and light chains with 5' and 3' Gibson overhangs were then cloned into human IgG1 and human kappa or lambda light chain expression vectors by Gibson assembly as previously described (53). The heavy and light chains of the corresponding mAb were cotransfected into HEK293T cells. After 4 days, mAbs secreted into the medium supernatant were harvested and purified using protein A-agarose beads (Thermo Fisher).

Recombinant proteins. The recombinant WT SARS-CoV-2 full-length (FL) spike, D614G FL spike, WT RBD, K417T/R/A RBD, N501Q/A RBD, and SARS-CoV-1 RBD and MERS-CoV were generated in-house either by using a gBlock fragment synthesized by Integrated DNA Technologies or by performing single-site mutagenesis and expressed by Expi293F cells (Thermo Fisher). The recombinant FL spikes derived from variants B.1.1.7, B.1.351, P.1, B.1.617.2, B.1.526, and B.1.617.1 were kindly provided by the Noah Sather laboratory at Seattle Children's Research Institute. The recombinant RBDs found in VOCs, B.1.351 or P.1 variants, and RBDs with single or multiple mutations (N439:Y453F, E406Q, K417E, K417V, Y453F, F486A, N487R, F490K, Q493R, N439K, N440K, and N501Y) were generously provided by the Kramer laboratory at the Icahn School of Medicine at Mount Sinai. The recombinant S1 and S2 subunits and RBDs with single mutations of K417N, E484K, and L452R were obtained from Sino Biological. The protein sequences and resources for each antigen are listed in Table S3.

Virus neutralization assay. Virus neutralization assays were performed with different variants of SARS-CoV-2 on Vero E6/TMPRSS2 cells (Table S4). Virus (~100 PFU) was incubated with an equal volume of 2-fold-diluted serum or mAbs for 1 h. Plasma samples were diluted in calcium-free medium, while antibodies were diluted in growth medium. In addition, plasma was heat treated for 30 min at 37°C prior to use. The antibody-virus mixture was added to confluent Vero E6/TMPRSS2 cells that were plated at 30,000 cells per well the previous day in 96-well plates. The cells were incubated for 3 days at 37°C and then fixed and stained with 20% methanol and a crystal violet solution. Virus neutralization titers were determined as the reciprocal of the highest serum dilution that completely prevented cytopathic effects. The 50% inhibitory concentrations (IC₅₀s) for mAbs were determined using the log(inhibitor) versus normalized response (variable slope), performed in Prism (version 9.0; GraphPad). All plasma and mAbs were tested in duplicate, and each experiment was performed twice.

Enzyme-linked immunosorbent assay. High-protein-binding microtiter plates (Costar) were coated with 50 μl of recombinant proteins (either full-length spike or the RBD) at 2 μg/ml in a 1× PBS solution overnight at 4°C. The plates were washed 3 times the next day with 1× PBS supplemented with 0.05% Tween 20 and blocked with 175 μl of 1× PBS containing 20% fetal bovine serum (FBS) for 1 h at 37°C. mAbs were serially diluted 1:3 starting at 10 μg/ml and incubated for 1 h at 37°C. The plates were then washed 3 times and incubated with horseradish peroxidase (HRP)-conjugated goat anti-human IgG antibody (Jackson ImmunoResearch) diluted 1:1,000 for 1 h at 37°C, and plates were subsequently developed with the Super AquaBlue enzyme-linked immunosorbent assay (ELISA) substrate (eBioscience). The absorbance was measured at 405 nm on a microplate spectrophotometer (Bio-Rad). To standardize the assays, control antibodies with known binding characteristics were included on each plate, and the plates were developed when the absorbance of the control reached 3.0 OD₄₀₅ (optical density at 405 nm) units. All mAbs were tested in duplicate, and each experiment was performed twice.

Competition ELISAs. To determine the classification of certain mAbs, competition ELISAs were carried out using the mAbs with known epitope binding properties as competitor mAbs. The competitor mAbs were biotinylated overnight at 4°C with EZ-Link sulfo-NHS-biotin (Thermo Scientific). The excess free biotin of biotinylated mAbs was removed with 7,000-molecular-weight-cutoff (MWCO) Zeba spin desalted columns (Thermo Scientific). Plates were coated with 50 μ l of 2 μ g/ml RBD antigen overnight at 4°C. After 1 h of blocking the plates with PBS–20% FBS, a 2-fold dilution of mAbs of an undetermined class or serum was added (starting at 20 μ g/ml of mAbs and a 1:50 dilution of serum) to the coated well. After incubation for 2 h at room temperature, the biotinylated competitor mAb was added at a concentration of $2 \times K_d$ (dissociation constant) and incubated for another 2 h at room temperature together with mAbs or serum that was previously added. The plates were washed 3 times and incubated with 100 μ l HRP-conjugated streptavidin (Southern Biotech) at a dilution of 1:1,000 for 1 h at 37°C. The plates were developed with the Super AquaBlue ELISA substrate (eBioscience). To standardize the assays, the competitor biotinylated mAb was added in a well without any competing mAbs or serum as a control well. The data were recorded when the absorbance of the control well reached 1 to 1.5 OD₄₀₅ units. All mAbs were tested in duplicate, and each experiment was performed twice. The percent competition was then calculated by dividing a sample's observed OD by the OD reached by the positive control, subtracting this value from 1, and multiplying by 100. For the serum data, ODs were log transformed and analyzed by nonlinear regression to determine 50% effective concentration (EC₅₀) values using Prism software (version 9.0; GraphPad).

Biolayer interferometry. To determine the classification of certain mAbs, competition assays were performed using mAbs with known epitope binding properties as competitor mAbs with a mAb binding unknown epitopes using biolayer interferometry (BLI) with an Octet K2 instrument (Forte Bio). The RBD of SARS-CoV-2 was biotinylated, desalted, and loaded at a concentration of 10 μ g/ml onto streptavidin probes for 300 s, followed by PBS for 60 s. The probe was moved to associate with mAbs of interest (10 μ g/ml) for 300 s, followed by PBS for 60 s and then associations with control mAbs (10 μ g/ml) for 300 s. The final volume for all the solutions was 200 μ l/well. All of the assays were performed with PBS buffer at 30°C.

SARS-CoV-2 spike and RBD protein models. FL mutations were visualized on the WT spike protein (PDB accession number 7KJ2) using PyMOL (Schrödinger). The models of RBD mutations and RBD classes were visualized on the WT RBD protein (PDB accession number 7KDL) using PyMOL (Schrödinger). The models were further processed by Adobe Illustrator 2021 and Adobe Photoshop.

Statistical analysis. All statistical analyses were performed using Prism software (version 9.0; GraphPad). Sample sizes for the number of mAbs tested are indicated in the corresponding figures or in the center of pie graphs. The numbers of biological repeats for experiments and specific tests for statistical significance used are indicated in the corresponding figure legends. *P* values of ≤ 0.05 were considered significant (*, *P* ≤ 0.05 ; **, *P* ≤ 0.01 ; ***, *P* ≤ 0.001 ; ****, *P* < 0.0001).

SUPPLEMENTAL MATERIAL

Supplemental material is available online only.

FIG S1, DOCX file, 1.3 MB.

FIG S2, DOCX file, 0.5 MB.

FIG S3, DOCX file, 0.2 MB.

TABLE S1, DOCX file, 0.03 MB.

TABLE S2, DOCX file, 0.03 MB.

TABLE S3, DOCX file, 0.03 MB.

TABLE S4, DOCX file, 0.03 MB.

ACKNOWLEDGMENTS

We kindly thank the University of Chicago CAT Facility (RRID SCR_017760) and the University of Chicago Genomics Facility (RRID SCR_019196) for assisting in sorting and sequencing samples. Finally, we appreciate the clinical staff at the University of Chicago Medicine Plasma Transfusion Program and the volunteers who participated in this study.

S.C. collected samples, designed experiments, sorted B cells, generated RNA sequencing libraries, generated mAb, generated recombinant antigens, analyzed the data, and wrote the manuscript. Y.F. designed and performed experiments, generated recombinant antigens, and wrote the manuscript. J.J.G. collected samples, designed and performed experiments, and wrote the manuscript. P.J.H., M.A., and W.R. performed virus neutralization assays. L.L. performed computational analyses of single-cell sequencing data. H.L.D. and C.T.S. collected samples, generated probes, sorted B cells, generated RNA sequencing libraries, and generated mAbs. N.-Y.Z. expressed mAbs. M.H. performed mAb cloning. J.W. performed serum ELISAs and expressed mAbs. S.A.E. generated probes and sorted B cells. H.A.U. performed ELISAs and expressed recombinant antigens. H.M.G. performed ELISAs. F.K. and F.A. produced and

provided recombinant SARS-CoV-2 RBD mutant antigens. D.N.S. provided recombinant variant SARS-CoV-2 spike antigens. Y.K. provided neutralization data. P.C.W. supervised the work and wrote the manuscript.

Several mAbs generated from this work are being used by Now Diagnostics in Springdale, AR, for the development of a diagnostic test. The University of Chicago has filed a patent application relating to anti-SARS-CoV-2 antibodies generated in previous work (27), with P.C.W., H.L.D., and C.T.S. as coinventors. The Icahn School of Medicine at Mount Sinai has filed patent applications relating to SARS-CoV-2 serological assays and NDV-based SARS-CoV-2 vaccines, which list F.K. as a coinventor. F.A. is also listed on the serological assay patent application as a coinventor. Mount Sinai has spun out a company, Kantaro, to market serological tests for SARS-CoV-2. F.K. has consulted for Merck and Pfizer (before 2020) and is currently consulting for Pfizer, Seqirus, and Avimex. The Krammer laboratory is also collaborating with Pfizer on animal models of SARS-CoV-2.

This project was funded in part by National Institute of Allergy and Infectious Diseases (NIAID), National Institutes of Health (NIH), grant numbers U19AI082724 (P.C.W.), U19AI109946 (P.C.W.), and U19AI057266 (P.C.W.) and NIAID Centers of Excellence for Influenza Research and Surveillance (CEIRS) grant number HHSN272201400005C (P.C.W.). F.K. and F.A. were funded by NIAID CEIRS contract HHSN272201400008C, Collaborative Influenza Vaccine Innovation Centers (CIVIC) contract 75N93019C00051, and the generous support of the JPB Foundation, the Open Philanthropy Project (number 2020-215611), and other philanthropic donations. Y.K. and P.J.H. were funded by the Research Program on Emerging and Re-emerging Infectious Diseases (JP19fk0108113, JP20fk0108272, and 20fk0108301); the Japan Program for Infectious Diseases Research and Infrastructure (JP20wm0125002) from the Japan Agency for Medical Research and Development (AMED); NIAID CEIRS contract HHSN272201400008C; and CIVIC contract 75N93019C00051. D.N.S. was funded by BEI/NIAID contract HHSN272201600013C.

REFERENCES

- Baden LR, El Sahly HM, Essink B, Kotloff K, Frey S, Novak R, Diemert D, Spector SA, Roupheal N, Creech CB, McGettigan J, Khetan S, Segall N, Solis J, Broz A, Fierro C, Schwartz H, Neuzil K, Corey L, Gilbert P, Janes H, Follmann D, Marovich M, Mascola J, Polakowski L, Ledgerwood J, Graham BS, Bennett H, Pajon R, Knightly C, Leav B, Deng W, Zhou H, Han S, Ivarsson M, Miller J, Zaks T. 2021. Efficacy and safety of the mRNA-1273 SARS-CoV-2 vaccine. *N Engl J Med* 384:403–416. <https://doi.org/10.1056/NEJMoa2035389>.
- Garcia-Beltran WF, Lam EC, St Denis K, Nitido AD, Garcia ZH, Hauser BM, Feldman J, Pavlovic MN, Gregory DJ, Poznansky MC, Sigal A, Schmidt AG, lafrate AJ, Naranbhai V, Balazs AB. 2021. Multiple SARS-CoV-2 variants escape neutralization by vaccine-induced humoral immunity. *Cell* 184:2372–2383.e9. <https://doi.org/10.1016/j.cell.2021.03.013>.
- Wang Z, Schmidt F, Weisblum Y, Muecksch F, Barnes CO, Finkin S, Schaefer-Babajew D, Cipolla M, Gaebler C, Lieberman JA, Oliveira TY, Yang Z, Abernathy ME, Huey-Tubman KE, Hurley A, Turroja M, West KA, Gordon K, Millard KG, Ramos V, Da Silva J, Xu J, Colbert RA, Patel R, Dizon J, Unson-O'Brien C, Shmeliovich I, Gazumyan A, Caskey M, Bjorkman PJ, Casellas R, Hatzioannou T, Bieniasz PD, Nussenzweig MC. 2021. mRNA vaccine-elicited antibodies to SARS-CoV-2 and circulating variants. *Nature* 592:616–622. <https://doi.org/10.1038/s41586-021-03324-6>.
- Wall EC, Wu M, Harvey R, Kelly G, Warchal S, Sawyer C, Daniels R, Hobson P, Hatipoglu E, Ngai Y, Hussain S, Nicod J, Goldstone R, Ambrose K, Hindmarsh S, Beale R, Riddell A, Gamblin S, Howell M, Kassiotis G, Libri V, Williams B, Swanton C, Gandhi S, Bauer DL. 2021. Neutralising antibody activity against SARS-CoV-2 VOCs B.1.617.2 and B.1.351 by BNT162b2 vaccination. *Lancet* 397:2331–2333. [https://doi.org/10.1016/S0140-6736\(21\)01290-3](https://doi.org/10.1016/S0140-6736(21)01290-3).
- Jiang SB, Hillyer C, Du LY. 2020. Neutralizing antibodies against SARS-CoV-2 and other human coronaviruses. *Trends Immunol* 41:355–359. <https://doi.org/10.1016/j.it.2020.03.007>.
- Korber B, Fischer WM, Gnanakaran S, Yoon H, Theiler J, Abfalterer W, Hengartner N, Giorgi EE, Bhattacharya T, Foley B, Hastie KM, Parker MD, Partridge DG, Evans CM, Freeman TM, de Silva TI, Sheffield COVID-19 Genomics Group, McDanal C, Perez LG, Tang H, Moon-Walker A, Whelan SP, LaBranche CC, Saphire EO, Montefiori DC. 2020. Tracking changes in SARS-CoV-2 spike: evidence that D614G increases infectivity of the COVID-19 virus. *Cell* 182:812–827.e19. <https://doi.org/10.1016/j.cell.2020.06.043>.
- Leung K, Shum MH, Leung GM, Lam TT, Wu JT. 2021. Early transmissibility assessment of the N501Y mutant strains of SARS-CoV-2 in the United Kingdom, October to November 2020. *Euro Surveill* 26:2002106. <https://doi.org/10.2807/1560-7917.ES.2020.26.1.2002106>.
- Liu H, Zhang Q, Wei P, Chen Z, Aviszus K, Yang J, Downing W, Jiang C, Liang B, Reynoso L, Downey GP, Frankel SK, Kappler J, Marrack P, Zhang G. 2021. The basis of a more contagious 501Y.V1 variant of SARS-CoV-2. *Cell Res* 31:720–722. <https://doi.org/10.1038/s41422-021-00496-8>.
- Volz E, Mishra S, Chand M, Barrett JC, Johnson R, Geidelberg L, Hinsley WR, Laydon DJ, Dabrera G, O'Toole Á, Amato R, Ragonnet-Cronin M, Harrison I, Jackson B, Ariani CV, Boyd O, Loman NJ, McCrone JT, Gonçalves S, Jorgensen D, Myers R, Hill V, Jackson DK, Gaythorpe K, Groves N, Sillitoe J, Kwiatkowski DP, COVID-19 Genomics UK (COG-UK) Consortium, Flaxman S, Ratmann O, Bhatt S, Hopkins S, Gandy A, Rambaut A, Ferguson NM. 2021. Assessing transmissibility of SARS-CoV-2 lineage B.1.1.7 in England. *Nature* 593:266–269. <https://doi.org/10.1038/s41586-021-03470-x>.
- Davies NG, Abbott S, Barnard RC, Jarvis CI, Kucharski AJ, Munday JD, Pearson CAB, Russell TW, Tully DC, Washburne AD, Wenseleers T, Gimma A, Waites W, Wong KLM, van Zandvoort K, Silverman JD, CMMID COVID-19 Working Group, COVID-19 Genomics UK (COG-UK) Consortium, Diaz-Ordaz K, Keogh R, Eggo RM, Funk S, Jit M, Atkins KE, Edmunds WJ. 2021. Estimated transmissibility and impact of SARS-CoV-2 lineage B.1.1.7 in England. *Science* 372:eabg3055. <https://doi.org/10.1126/science.abg3055>.
- Annavaiahala MK, Mohri H, Wang P, et al. 2021. Emergence and expansion of SARS-CoV-2 B.1.526 after identification in New York. *Nature* 597:703–708. <https://doi.org/10.1038/s41586-021-03908-2>.
- Nonaka CKV, Franco MM, Gräf T, de Lorenzo Barcia CA, de Ávila Mendonça RN, de Sousa KAF, Neiva LMC, Fosenca V, Mendes AVA, de Aguiar RS, Giovanetti M, de Freitas Souza BS. 2021. Genomic evidence of SARS-CoV-2

- reinfection involving E484K spike mutation, Brazil. *Emerg Infect Dis* 27: 1522–1524. <https://doi.org/10.3201/eid2705.210191>.
13. Tegally H, Wilkinson E, Lessells RJ, Giandhari J, Pillay S, Msomi N, Mlisana K, Bhiman JN, von Gottberg A, Walaza S, Fonseca V, Allam M, Ismail A, Glass AJ, Engelbrecht S, Van Zyl G, Preiser W, Williamson C, Petruccione F, Sigal A, Gazy I, Hardie D, Hsiao N-Y, Martin D, York D, Goedhals D, San EJ, Giovanetti M, Lourenço J, Alcantara LCJ, de Oliveira T. 2021. Sixteen novel lineages of SARS-CoV-2 in South Africa. *Nat Med* 27:440–446. <https://doi.org/10.1038/s41591-021-01255-3>.
 14. Hirotsu Y, Omata M. 2021. Detection of R.1 lineage severe acute respiratory syndrome coronavirus 2 (SARS-CoV-2) with spike protein W152L/E484K/G769V mutations in Japan. *PLoS Pathog* 17:e1009619. <https://doi.org/10.1371/journal.ppat.1009619>.
 15. Edara V-V, Lai L, Sahoo MK, Floyd K, Sibai M, Solis D, Flowers MW, Hussaini L, Ciric CR, Bechnack S, Stephens K, Mokhtari EB, Mudvari P, Creanga A, Pegu A, Derrien-Coleman A, Henry AR, Gagne M, Graham BS, Wrammert J, Douek DC, Boritz E, Pinsky BA, Suthar MS. 2021. Infection and vaccine-induced neutralizing-antibody responses to the SARS-CoV-2 B.1.617 variants. *N Engl J Med* 385:664–666. <https://doi.org/10.1056/NEJMc2107799>.
 16. Shang J, Ye G, Shi K, Wan Y, Luo C, Aihara H, Geng Q, Auerbach A, Li F. 2020. Structural basis of receptor recognition by SARS-CoV-2. *Nature* 581: 221–224. <https://doi.org/10.1038/s41586-020-2179-y>.
 17. Yuan M, Liu HJ, Wu NIC, Wilson IA. 2021. Recognition of the SARS-CoV-2 receptor binding domain by neutralizing antibodies. *Biochem Biophys Res Commun* 538:192–203. <https://doi.org/10.1016/j.bbrc.2020.10.012>.
 18. Zhou D, Dejnirattisai W, Supasa P, Liu C, Mentzer AJ, Ginn HM, Zhao Y, Duyvesteyn HME, Tuekprakhon A, Nutalai R, Wang B, Paesen GC, Lopez-Camacho C, Slon-Campos J, Hallis B, Coombes N, Bewley K, Charlton S, Walter TS, Skelly D, Lumley SF, Dold C, Levin R, Dong T, Pollard AJ, Knight JC, Crook D, Lambe T, Clutterbuck E, Bibi S, Flaxman A, Bittaye M, Belij-Rammerstorfer S, Gilbert S, James W, Carroll MW, Klenerman P, Barnes E, Dunachie SJ, Fry EE, Mongkolsapaya J, Ren J, Stuart DI, Screaton GR. 2021. Evidence of escape of SARS-CoV-2 variant B.1.351 from natural and vaccine-induced sera. *Cell* 184:2348–2361.e6. <https://doi.org/10.1016/j.cell.2021.02.037>.
 19. Plante JA, Mitchell BM, Plante KS, Debbink K, Weaver SC, Menachery VD. 2021. The variant gambit: COVID-19's next move. *Cell Host Microbe* 29: 508–515. <https://doi.org/10.1016/j.chom.2021.02.020>.
 20. Yadav PD, Sapkal GN, Abraham P, Ella R, Deshpande G, Patil DY, Nyayanit DA, Gupta N, Sahay RR, Shete AM, Panda S, Bhargava B, Mohan VK. 7 May 2021. Neutralization of variant under investigation B.1.617 with sera of BBV152 vaccinees. *Clin Infect Dis* <https://doi.org/10.1093/cid/ciab411>.
 21. Singh J, Rahman SA, Ehtesham NZ, Hira S, Hasnain SE. 2021. SARS-CoV-2 variants of concern are emerging in India. *Nat Med* 27:1131–1133. <https://doi.org/10.1038/s41591-021-01397-4>.
 22. World Health Organization. 2021. COVID-19 weekly epidemiological update, edition 43, 8 June 2021. World Health Organization, Geneva, Switzerland.
 23. Lopez Bernal J, Andrews N, Gower C, Gallagher E, Simmons R, Thelwall S, Stowe J, Tessier E, Groves N, Dabrera G, Myers R, Campbell C, Amirthalingam G, Edmunds M, Zambon M, Brown K, Hopkins S, Chand M, Ramsay M. 2021. Effectiveness of Covid-19 vaccines against the B.1.617.2 (Delta) variant. *N Engl J Med* 385:585–594. <https://doi.org/10.1056/NEJMoa2108891>.
 24. Saito A, Nasser H, Uriu K, Kosugi Y, Irie T, Shirakawa K, Sadamasu K, Kimura I, Ito J, Wu J, Ozono S, Tokunaga K, Butlertanaka EP, Tanaka YL, Shimizu R, Shimizu K, Fukuhara T, Kawabata R, Sakaguchi T, Yoshida I, Asakura H, Nagashima M, Yoshimura K, Kazuma Y, Nomura R, Horisawa Y, Takaori-Kondo A, The Genotype to Phenotype Japan (G2P-Japan) Consortium, Nakagawa S, Ikeda T, Sato K. 2021. SARS-CoV-2 spike P681R mutation enhances and accelerates viral fusion. *bioRxiv* <https://doi.org/10.1101/2021.06.17.448820>.
 25. Bugembe DL, Phan MVT, Ssewanyana I, et al. 2021. Emergence and spread of a SARS-CoV-2 lineage A variant (A.23.1) with altered spike protein in Uganda. *Nat Microbiol* 6:1094–1101. <https://doi.org/10.1038/s41564-021-00933-9>.
 26. Guthmiller JJ, Stovicek O, Wang J, Changrob S, Li L, Halfmann P, Zheng N-Y, Utset H, Stamper CT, Dugan HL, Miller WD, Huang M, Dai Y-N, Nelson CA, Hall PD, Jansen M, Shanmugarajah K, Donington JS, Krammer F, Fremont DH, Joachimiak A, Kawaoka Y, Tesic V, Madariaga ML, Wilson PC. 2021. SARS-CoV-2 infection severity is linked to superior humoral immunity against the spike. *mbio* 12:e02940-20. <https://doi.org/10.1128/mbio.02940-20>.
 27. Dugan HL, Stamper CT, Li L, Changrob S, Asby NW, Halfmann PJ, Zheng N-Y, Huang M, Shaw DG, Cobb MS, Erickson SA, Guthmiller JJ, Stovicek O, Wang J, Winkler ES, Madariaga ML, Shanmugarajah K, Jansen MO, Amanat F, Stewart I, Utset HA, Huang J, Nelson CA, Dai Y-N, Hall PD, Jedrzejczak RP, Joachimiak A, Krammer F, Diamond MS, Fremont DH, Kawaoka Y, Wilson PC. 2021. Profiling B cell immunodominance after SARS-CoV-2 infection reveals antibody evolution to non-neutralizing viral targets. *Immunity* 54: 1290–1303.e7. <https://doi.org/10.1016/j.immuni.2021.05.001>.
 28. Ju B, Zhang Q, Ge J, Wang R, Sun J, Ge X, Yu J, Shan S, Zhou B, Song S, Tang X, Yu J, Lan J, Yuan J, Wang H, Zhao J, Zhang S, Wang Y, Shi X, Liu L, Zhao J, Wang X, Zhang Z, Zhang L. 2020. Human neutralizing antibodies elicited by SARS-CoV-2 infection. *Nature* 584:115–119. <https://doi.org/10.1038/s41586-020-2380-z>.
 29. Zost SJ, Gilchuk P, Case JB, Binshtein E, Chen RE, Nkolola JP, Schäfer A, Reidy JX, Trivette A, Nargi RS, Sutton RE, Suryadevara N, Martinez DR, Williamson LE, Chen EC, Jones T, Day S, Myers L, Hassan AO, Kafai NM, Winkler ES, Fox JM, Shrihari S, Mueller BK, Meiler J, Chandrashekar A, Mercado NB, Steinhardt JJ, Ren K, Loo Y-M, Kallewaard NL, McCune BT, Keeler SP, Holtzman MJ, Barouch DH, Gralinski LE, Baric RS, Thackray LB, Diamond MS, Carnahan RH, Crowe JE, Jr. 2020. Potently neutralizing and protective human antibodies against SARS-CoV-2. *Nature* 584:443–449. <https://doi.org/10.1038/s41586-020-2548-6>.
 30. Greaney AJ, Starr TN, Barnes CO, et al. 2021. Mapping mutations to the SARS-CoV-2 RBD that escape binding by different classes of antibodies. *Nat Commun* 12:4196. <https://doi.org/10.1038/s41467-021-24435-8>.
 31. Starr TN, Greaney AJ, Addetia A, Hannon WW, Choudhary MC, Dings AS, Li JZ, Bloom JD. 2021. Prospective mapping of viral mutations that escape antibodies used to treat COVID-19. *Science* 371:850–854. <https://doi.org/10.1126/science.abb9302>.
 32. Greaney AJ, Starr TN, Gilchuk P, Zost SJ, Binshtein E, Loes AN, Hilton SK, Huddleston J, Eguia R, Crawford KHD, Dings AS, Nargi RS, Sutton RE, Suryadevara N, Rothlauf PW, Liu Z, Whelan SPJ, Carnahan RH, Crowe JE, Jr, Bloom JD. 2021. Complete mapping of mutations to the SARS-CoV-2 spike receptor-binding domain that escape antibody recognition. *Cell Host Microbe* 29:44–57.e9. <https://doi.org/10.1016/j.chom.2020.11.007>.
 33. Lan J, Ge J, Yu J, Shan S, Zhou H, Fan S, Zhang Q, Shi X, Wang Q, Zhang L, Wang X. 2020. Structure of the SARS-CoV-2 spike receptor-binding domain bound to the ACE2 receptor. *Nature* 581:215–220. <https://doi.org/10.1038/s41586-020-2180-5>.
 34. Starr TN, Greaney AJ, Hilton SK, Ellis D, Crawford KHD, Dings AS, Navarro MJ, Bowen JE, Tortorici MA, Walls AC, King NP, Veeler D, Bloom JD. 2020. Deep mutational scanning of SARS-CoV-2 receptor binding domain reveals constraints on folding and ACE2 binding. *Cell* 182:1295–1310.e20. <https://doi.org/10.1016/j.cell.2020.08.012>.
 35. Weisblum Y, Schmidt F, Zhang F, DaSilva J, Poston D, Lorenzi JCC, Muecksch F, Rutkowska M, Hoffmann H-H, Michailidis E, Gaebler C, Agudelo M, Cho A, Wang Z, Gazumyan A, Cipolla M, Luchsinger L, Hillier CD, Caskey M, Robbiani DF, Rice CM, Nussenzweig MC, Hatziioannou T, Bieniasz PD. 2020. Escape from neutralizing antibodies by SARS-CoV-2 spike protein variants. *Elife* 9:e61312. <https://doi.org/10.7554/eLife.61312>.
 36. Barnes CO, Jette CA, Abernathy ME, Dam K-MA, Esswein SR, Gristick HB, Malyutin AG, Sharaf NG, Huey-Tubman KE, Lee YE, Robbiani DF, Nussenzweig MC, West AP, Bjorkman PJ. 2020. SARS-CoV-2 neutralizing antibody structures inform therapeutic strategies. *Nature* 588:682–687. <https://doi.org/10.1038/s41586-020-2852-1>.
 37. Yuan M, Liu H, Wu NC, Lee C-CD, Zhu X, Zhao F, Huang D, Yu W, Hua Y, Tien H, Rogers TF, Landais E, Sok D, Jardine JG, Burton DR, Wilson IA. 2020. Structural basis of a shared antibody response to SARS-CoV-2. *Science* 369:1119–1123. <https://doi.org/10.1126/science.abd2321>.
 38. Cherian S, Potdar V, Jadhav S, Yadav P, Gupta N, Das M, Rakshit P, Singh S, Abraham P, Panda S, Nic Team. 2021. SARS-CoV-2 spike mutations, L452R, T478K, E484Q and P681R, in the second wave of COVID-19 in Maharashtra, India. *Microorganisms* 9:1542. <https://doi.org/10.3390/microorganisms9071542>.
 39. Thomson EC, Rosen LE, Shepherd JG, Spreafico R, da Silva Filipe A, Wojcechowskyj JA, Davis C, Piccoli L, Pascall DJ, Dillen J, Lytras S, Czudnochowski N, Shah R, Meury M, Jesudason N, De Marco A, Li K, Bassi J, O'Toole A, Pinto D, Colquhoun RM, Culap K, Jackson B, Zatta F, Rambaut A, Jacoani S, Sreenu VB, Nix J, Zhang I, Jarrett RF, Glass WG, Beltramello M, Nomikou K, Pizzuto M, Tong L, Cameroni E, Croll TI, Johnson N, Di Iulio J, Wickenhagen A, Ceschi A, Harbison AM, Mair D, Ferrari P, Smollett K, Sallusto F, Carmichael S, Garzoni C, Nichols J, Galli M, et al. 2021. Circulating SARS-CoV-2 spike N439K variants maintain fitness while evading antibody-mediated immunity. *Cell* 184:1171–1187.e20. <https://doi.org/10.1016/j.cell.2021.01.037>.
 40. Deng X, Garcia-Knight MA, Khalid MM, Servellita V, Wang C, Morris MK, Sotomayor-González A, Glasner DR, Reyes KR, Gliwa AS, Reddy NP, Sanchez

- San Martin C, Federman S, Cheng J, Balcerak J, Taylor J, Streithorst JA, Miller S, Sreekumar B, Chen PY, Schulze-Gahmen U, Taha TY, Hayashi JM, Simoneau CR, Kumar GR, McMahan S, Lidsky PV, Xiao Y, Hemarajata P, Green NM, Espinosa A, Kath C, Haw M, Bell J, Hacker JK, Hanson C, Wadford DA, Anaya C, Ferguson D, Frankino PA, Shivram H, Lareau LF, Wyman SK, Ott M, Andino R, Chiu CY. 2021. Transmission, infectivity, and neutralization of a spike L452R SARS-CoV-2 variant. *Cell* 184(13):3426–3437.e8. <https://doi.org/10.1016/j.cell.2021.04.025>.
41. Galson JD, Schaetzle S, Bashford-Rogers RJM, Raybould MJ, Kovaltsuk A, Kilpatrick GJ, Minter R, Finch DK, Dias J, James LK, Thomas G, Lee W-YJ, Betley J, Cavlan O, Leech A, Deane CM, Seoane J, Caldas C, Pennington DJ, Pfeffer P, Osbourn J. 2020. Deep sequencing of B cell receptor repertoires from COVID-19 patients reveals strong convergent immune signatures. *Front Immunol* 11:605170. <https://doi.org/10.3389/fimmu.2020.605170>.
 42. Robbiani DF, Gaebler C, Muecksch F, Lorenzi JCC, Wang Z, Cho A, Agudelo M, Barnes CO, Gazumy A, Finkin S, Högglöf T, Oliveira TY, Viant C, Hurley A, Hoffmann H-H, Millard KG, Kost RG, Cipolla M, Gordon K, Bianchini F, Chen ST, Ramos V, Patel R, Dizon J, Shimeliovich I, Mendoza P, Hartweger H, Nogueira L, Pack M, Horowitz J, Schmidt F, Weisblum Y, Michailidis E, Ashbrook AW, Waltari E, Pak JE, Huey-Tubman KE, Koranda N, Hoffman PR, West AP, Rice CM, Hatziioannou T, Bjorkman PJ, Bieniasz PD, Caskey M, Nussenzweig MC. 2020. Convergent antibody responses to SARS-CoV-2 in convalescent individuals. *Nature* 584:437–442. <https://doi.org/10.1038/s41586-020-2456-9>.
 43. Schmitz AJ, Turner JS, Liu Z, Zhou JQ, Aziati ID, Chen RE, Joshi A, Bricker TL, Darling TL, Adelsberg DC, Altomare CG, Alsoussi WB, Case JB, VanBlargan LA, Lei T, Thapa M, Amanat F, Jeevan T, Fabrizio T, O'Halloran JA, Shi PY, Presti RM, Webby RJ, Krammer F, Whelan SPJ, Bajic G, Diamond MS, Boon ACM, Ellebedy AH. 2021. A vaccine-induced public antibody protects against SARS-CoV-2 and emerging variants. *Immunity* 54(9): 2159–2166.e6. <https://doi.org/10.1016/j.immuni.2021.08.013>.
 44. Faria NR, Mellan TA, Whittaker C, Claro IM, Candido DDS, Mishra S, Crispim MAE, Sales FCS, Hawryluk I, McCrone JT, Hulswit RJG, Franco LAM, Ramundo MS, de Jesus JG, Andrade PS, Coletti TM, Ferreira GM, Silva CAM, Manuli ER, Pereira RHM, Peixoto PS, Kraemer MUG, Gaburo N, Jr, Camilo CDC, Hoeltgebaum H, Souza WM, Rocha EC, de Souza LM, de Pinho MC, Araujo LJ, Malta FSV, de Lima AB, Silva JDP, Zauli DAG, Ferreira ACDS, Schnekenberg RP, Laydon DJ, Walker PGT, Schlüter HM, Dos Santos ALP, Vidal MS, Del Caro VS, Filho RMF, dos Santos HM, Aguiar RS, Proença-Modena JL, Nelson B, Hay JA, Monod M, Miscouridou X, et al. 2021. Genomics and epidemiology of the P.1 SARS-CoV-2 lineage in Manaus, Brazil. *Science* 372:815–821. <https://doi.org/10.1126/science.abh2644>.
 45. Amanat F, Thapa M, Lei T, Ahmed SMS, Adelsberg DC, Carreño JM, Strohmeier S, Schmitz AJ, Zafar S, Zhou JQ, Rijnik W, Alshammari H, Borchering N, Reiche AG, Srivastava K, Sordillo EM, van Bakel H, Turner JS, Bajic G, Simon V, Ellebedy AH, Krammer F, Ahmed B, Altman D, Amoako A, Awawda M, Beach K, Bermúdez-González C, Chernet R, Eaker L, Fabre S, Ferreri ED, Floda D, Gleason C, Kleiner G, Jurczynszak D, Matthews J, Mendez W, Mulder LCF, Polanco J, Russo K, Salimbangon A, Saksena M, Shin AS, Sominsky L, Suthakaran S, Wajnberg A. 2021. SARS-CoV-2 mRNA vaccination induces functionally diverse antibodies to NTD, RBD and S2. *Cell* 184: 3936–3948.e10. <https://doi.org/10.1016/j.cell.2021.06.005>.
 46. Chi X, Yan R, Zhang J, Zhang G, Zhang Y, Hao M, Zhang Z, Fan P, Dong Y, Yang Y, Chen Z, Guo Y, Zhang J, Li Y, Song X, Chen Y, Xia L, Fu L, Hou L, Xu J, Yu C, Li J, Zhou Q, Chen W. 2020. A neutralizing human antibody binds to the N-terminal domain of the spike protein of SARS-CoV-2. *Science* 369:650–655. <https://doi.org/10.1126/science.abc6952>.
 47. Ng KW, Faulkner N, Cornish GH, Rosa A, Harvey R, Hussain S, Ulferts R, Earl C, Wrobel AG, Benton DJ, Roustan C, Bolland W, Thompson R, Agua-Doce A, Hobson P, Heaney J, Rickman H, Paraskevopoulou S, Houlihan CF, Thomson K, Sanchez E, Shin GY, Spyer MJ, Joshi D, O'Reilly N, Walker PA, Kjaer S, Riddell A, Moore C, Jebson BR, Wilkinson M, Marshall LR, Rosser EC, Radziszewska A, Peckham H, Ciurtin C, Wedderburn LR, Beale R, Swanton C, Gandhi S, Stockinger B, McCauley J, Gamblin SJ, McCoy LE, Cherepanov P, Nastouli E, Kassiotis G. 2020. Preexisting and de novo humoral immunity to SARS-CoV-2 in humans. *Science* 370:1339–1343. <https://doi.org/10.1126/science.abe1107>.
 48. Shrock E, Fujimura E, Kula T, Timms RT, Lee I-H, Leng Y, Robinson ML, Sie BM, Li MZ, Chen Y, Logue J, Zuiani A, McCulloch D, Leis FJN, Henson S, Monaco DR, Travers M, Habibi S, Clarke WA, Caturegli P, Laeyendecker O, Piechocka-Trocha A, Li JZ, Khatri A, Chu HY, MGH COVID-19 Collection & Processing Team, Villani A-C, Kays K, Goldberg MB, Hachohen N, Filbin MR, Yu XG, Walker BD, Wesemann DR, Larman HB, Lederer JA, Elledge SJ. 2020. Viral epitope profiling of COVID-19 patients reveals cross-reactivity and correlates of severity. *Science* 370:eabd4250. <https://doi.org/10.1126/science.abd4250>.
 49. Chan CEZ, Seah SGK, Chye DH, Massey S, Torres M, Lim APC, Wong SKK, Neo JYJ, Wong PS, Lim JH, Loh GSL, Wang D, Boyd-Kirkup JD, Guan S, Thakkar D, Teo GH, Purushotorman K, Hutchinson PE, Young BE, Low JG, MacAry PA, Hentze H, Prativadibhayankara VS, Ethirajulu K, Comer JE, Tseng C-TK, Barrett ADT, Ingram PJ, Brasel T, Hanson BJ. 2021. The Fc-mediated effector functions of a potent SARS-CoV-2 neutralizing antibody, SC31, isolated from an early convalescent COVID-19 patient, are essential for the optimal therapeutic efficacy of the antibody. *PLoS One* 16:e0253487. <https://doi.org/10.1371/journal.pone.0253487>.
 50. Cao Y, Su B, Guo X, Sun W, Deng Y, Bao L, Zhu Q, Zhang X, Zheng Y, Geng C, Chai X, He R, Li X, Lv Q, Zhu H, Deng W, Xu Y, Wang Y, Qiao L, Tan Y, Song L, Wang G, Du X, Gao N, Liu J, Xiao J, Su X-D, Du Z, Feng Y, Qin C, Qin C, Jin R, Xie XS. 2020. Potent neutralizing antibodies against SARS-CoV-2 identified by high-throughput single-cell sequencing of convalescent patients' B cells. *Cell* 182:73–84.e16. <https://doi.org/10.1016/j.cell.2020.05.025>.
 51. Stuart T, Butler A, Hoffman P, Hafemeister C, Papalexi E, Mauck WM, Jr, Hao Y, Stoekius M, Smibert P, Satija R. 2019. Comprehensive integration of single-cell data. *Cell* 177:1888–1902.e21. <https://doi.org/10.1016/j.cell.2019.05.031>.
 52. Ye J, Ma N, Madden TL, Ostell JM. 2013. IgBLAST: an immunoglobulin variable domain sequence analysis tool. *Nucleic Acids Res* 41:W34–W40. <https://doi.org/10.1093/nar/gkt382>.
 53. Guthmiller JJ, Dugan HL, Neu KE, Lan LY, Wilson PC. 2019. An efficient method to generate monoclonal antibodies from human B cells. *Methods Mol Biol* 1904:109–145. https://doi.org/10.1007/978-1-4939-8958-4_5.